AALBORG UNIVERSITET
STUDENTERRAPPORT

Thermal imaging as method of studying vasomotion

7. Semester project - Fall 2017

Group 7407

AALBORG UNIVERSITET
STUDENTERRAPPORT

Title:
Thermal imaging as method of studying vasomotion

Theme:
Don't know

Project period:
P7, Fall 2017
01/09/2017 - 20/12/2017

Projektgruppe:
17gr7407

Students:
Annabel Bantle
Toby Steven Waterstone
Christian Korfitz Mortensen

Supervisors:
Lasse Østergaard
Caraten Dahl Mørch
Andrei Ciubotariu

Pages: ??
Appendix: ??
Handed in: 20/12/2017

7th Semester, Project

School of Medicine and Health

Biomedical Engineering and Informatics

Fredrik Bajers Vej 7A

9220 Aalborg

Synopsis

To be written

Abstract

also needs to be written

Preface

Needs to be written

-Tell about us as group, the place we study, something about the study
-Thank the supervisors

Contents

Part I

Background

1 | Anatomy and Physiology

The following chapter outlines the functions of the cardiovascular system and focuses on its microcirculatory part. Further the phenomena of vasomotion is illustrated.

1.1 Macrocirculatory system

The main function of the cardiovascular system is the blood supply of the whole body and the transportation of metabolites. The propulsion of this is the heart. It generates the systolic blood pressure through the strength of left ventricle. The pressure difference between the heart and the periphery emerging from there, ensures the blood flow. The blood flows from regions with high pressure, like the aorta, to regions with low pressure, like the periphery.[1]

The heart supplies the body through the systemic and the pulmonary circuit with blood. Through these circuits the heart regulates the blood allocation with adjustment of stroke volume and heart frequency. The oxygen-rich blood accumulates in the left ventricle. From there the blood is pushed out through the aortic valve into the aorta and via the arteries spread into the whole body. The venous system returns the meanwhile low in oxygen blood back to the heart into the right atrium. From there the blood flows into the right ventricle and is pushed out through the pulmonary valve into the lung arteries. In the lungs gas exchange of the blood happens. Subsequent the oxygen-rich blood flows via the pulmonary veins back to the left heart to supply the body.[1]

As mentioned, there are two types of vessels, arteries and veins. The difference between those two types of vessels is that arteries transport the blood away from the heart and veins solely transport blood to the heart. There are also some differences in the structure of arteries and veins. Arteries consist of three different layers, tunica interna, tunica media and tunica externa. The tunica interna consists of vascular endothelium, the tunica media consists of smooth muscle cells and elastic fibres, the tunica externa consists of connective tissue and also elastic fibres. Furthermore, there are two different types of arterial vessels. In arteries of the elastic type prevail the elastic fibres in the tunica media. This allows an abrupt extension of the vessel during the systole and ensuing constriction, due to this the blood is transported. This phenomena is called windkessel function. In arteries of the muscular type prevail the muscular fibres in the tunica media. This allows regulation of the lumen by constriction and dilatation, whereby the resistance and the blood flow in the organs is regulated.[1]

Venous vessels are similarly structured like arterial vessels, however they are thinner and have also semilunar valves inside, to inhibit back flow inside the vessels. This system is supported by the skeletal muscles which help to hold up blood flow. The arterial and the venous vessel system are connected through the capillary system in the microcirculatory

system.[1]

1.2 Microcirculatory system

The heart and larger arteries and veins are associated with the cardiovascular system, but those are only used for transportation of blood. Instead it is the capillaries, that permeate most tissues, that is responsible for the perfusion of tissue. These are the only vessels which permit exchange between the vessel and the surrounding interstitial fluids. Factors that affect tissue perfusion is cardiac output, peripheral resistance and blood pressure. Capillaries are made not of single individual fluid conductors like veins and arteries, but instead formed into capillary beds. Here they work as a interconnected network of vessels. As mentioned before the arteries decrease in size the further they expand into the peripheral system. The small arteries divide into arterioles which further divide into dozen of capillaries. The capillaries merge into a venule after the blood has been de-oxygenated. A capillary is divided into two segments, first the metarteriole and second the capillary. The blood flow between arterioles and venules can also be a direct connection, made by an arteriovenous anastomosis. This works as a bypass diverting blood flow around the capillary bed. An example of the structure of the capillary bed can be seen on fig. 1.1.[1]

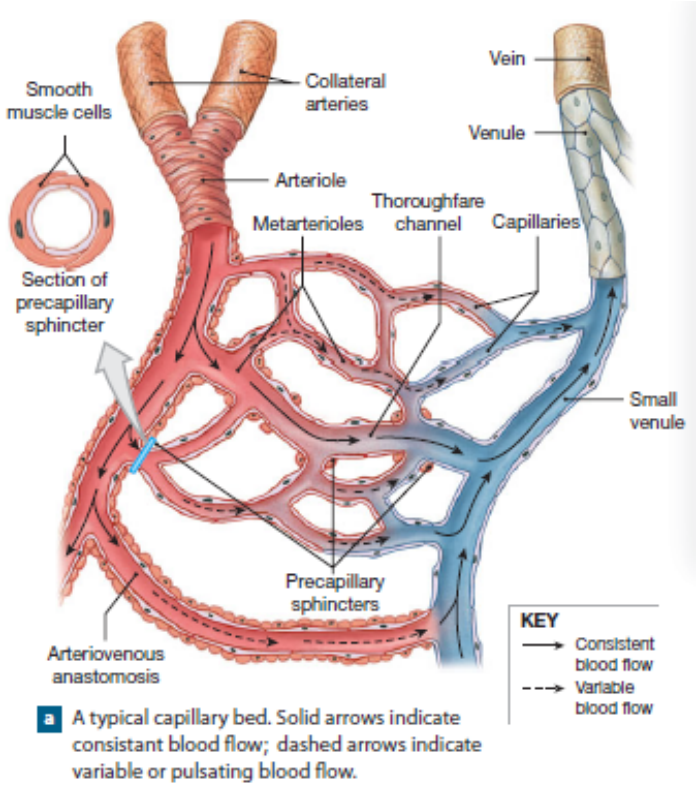

Figure 1.1: The basic structure of a capillary bed, with arteriole on the left side of the bed and a venule on the right[1].

Each capillary entrance is controlled by a precapillary sphincter, which is composed of smooth muscle cells, that are able to contract or relax and thereby limit access of blood flow to certain capillaries. The blood flows relatively slow within the capillaries giving time for the two way exchange of nutrients and wastes. [1]

1.2.1 Vasomotion

The flow within the capillaries varies. This is among other thing due to the earlier mentioned precapillary sphincters opening and closing. The opening and closing of sphincters is part of the autoregulation process performed at a local level, to control the blood flow. The vascular system does not contain blood enough for every vessel a capillary beds to be filled with blood. Therefore only 25% of the vessels in a capillary bed contains blood, and vessels activity needs to be well coordinated. Thermoregulation and control of nutrition balance are the primary functions of the microcirculatory system. Local changes in concentration of chemicals and interstitial fluids eg. dissolved oxygen concentrations in tissue modulates the vascular smooth muscles activity. Constriction and dilation of the vessel is thereby regulated by this periodic activity, also known as vasomotion. [1, 2]

Under normal circumstances cardiac output remains stable and the control of local blood flow happens through local peripheral resistance within local tissues. The regulation of cardiovascular activity is controlled by local homeostatic mechanism. These make sure that demands such as oxygen and nutrients are meet and wastes are disposed.[1]

Physiological mechanism controlling vasomotion are not yet fully understood, but vascular smooth muscle activity has been shown to be roughly proportional to the tissue's metabolic demand for oxygen.[2] Further have some factors that trigger homeostatic mechanism to alter the vasomotion been said to have an impact. Factors that trigger dilation is called vasodilators and can be some of the following:[1, 2]

- Decreased oxygen level or increased CO2 level
- Lactic acid or other acids generated from tissue cells
- Nitric oxide NO released from endothelial cells
- Rising concentrations of potassium ions or hydrogen ions in the interstitial fluid
- Chemicals released during local inflammation
- Elevated local temperature

A vasodialation will result in increased oxygen, nitrients, buffers released to recreate homeostasis. Factors that stimulate contriction is called vasoconstricters and can happen due to following:[1]

- Damaged tissue
- Aggregating platelets

2 | Hemodynamics

Hemodynamics explains the movement or flow of blood. It is influenced by parameters like blood pressure, blood volume, cardiac output, blood composition, etc. It is possible to measure some of the hemodynamic parameters non-invasive, and also to calculate parameters.[1, 3]

2.1 Physiological Base

The regulation of the blood pressure happens with baroreceptors in the walls of the big arteries in chest and neck area. These receptors register the changes of the elongation of the vessels and transmit this information to medulla oblongata. With the received pressure informations initiates the medulla oblongata, if necessary, regulatory measures. For the short-term regulation is the sympathicus responsible. Both, middle-term and long-term regulation, is made by the kidneys. For middle-term regulation messenger substance are released, which entail vasoconstriction. The long-term regulation occurs per pressure diuresis or reabsorption in the kidneys.It is possible to measure different blood pressures at different places in the cardiovascular system, for example the mean arterial pressure (MAP). The MAP increases in relation to the stroke volume and decreases when blood flows into the peripheral system. The central venous pressure (CVP) states the pressure in the venous system and complies approximately the pressure in the right ventricle. CVP depends on the filling volume of the venous system. Cardiac output, total periphery resistance and the viscosity of blood affect the blood pressure.[1, 3]

The cardiac output (CO) states the blood volume, which is pumped by the heart per time unit (HR). The calculation of the CO as follows.[1]

$$CO = HR \times strokevolume \tag{2.1}$$

The total periphery resistance (TPR) is the flow resistance of the systemic circulation and results from the sum of all vessel resistances. TPR depends on MAP , CVP and CO. [1]

$$TPR = \frac{MAP - CVP}{CO} \tag{2.2}$$

2.2 Physical Base

To consider the hemodynamics, it is possible to draw conclusions by analogy of physical laws. Especially of Ohm's law $R = \frac{U}{I}$ or rather $I = \frac{U}{R}$. A special case of Ohm's law

constitutes Hagen-Poiseuille's law in the field of fluid dynamic and rheology. Hagen-Poiseuille's law describes the laminar flow of an homogeneous Newtonian fluid through a rigid pipe depending on characteristics of the fluid and of the pipe.[4, 3]

Blood is an inhomogeneous suspension of liquid and corpuscular components, whose viscosity η depends on more factors than the temperature, and is consequently no Newtonian fluid. Nevertheless it is possible to draw conclusions by analogy out of Hagen-Poiseuille's law for the computation of the hemodynamics.[4, 3]

$$\frac{V}{t} = \frac{r^4 \times \pi \times \Delta P}{8 \times \eta \times I} \tag{2.3}$$

Here is the volume flow equivalent to the electrical current I and the pressure difference ΔP to the electric voltage U. Thus, the calculation of the resistance as follows.[4, 3]

$$R = \frac{8 \times I \times \eta}{r^4} \tag{2.4}$$

Thereby volume flow increases 16 times and the resistance decreases 16 times for double radius r.[4, 3]

In the blood, oxygen is tied to a large extent by hemoglobin. The oxygen saturation (sO_2) describes the percentage of the oxygenated hemoglobin. With rising oxygen partial pressure (pO_2) increases the oxygen saturation. This relation between sO_2 and pO_2 is showed by the oxygen binding curve.[1, 5]

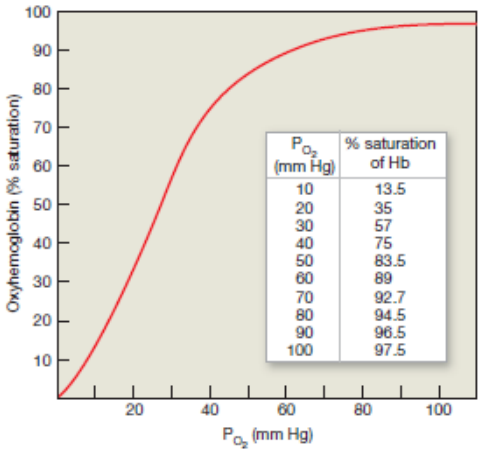

Figure 2.1: The oxygen binding curve shows the relation between sO_2 and pO_2 [1].

The oxygen content (cO_2) of the blood depends on both, the oxygen saturation and the oxygen partial pressure. cO_2 is calculated by the sum of the hemoglobin bounded and the

physical dissolved oxygen.[1, 5]

$$cO_2 = Hb \times 1,34\frac{ml}{g} + pO_2 \times 0,003\frac{ml \times dl}{mmHg} \tag{2.5}$$

The available oxygen (DO_2) is calculated by the oxygen content of the blood and the cardiac output.[1, 5]

$$DO_2 = cO_2 \times CO \tag{2.6}$$

The consumption of oxygen (VO_2) is calculated by the difference between the available oxygen in the arterial and the venous blood and the cardiac output.[1, 5]

$$VO_2 = (c_aO_2 - c_vO_2) \times CO \tag{2.7}$$

Therefore one can draw a conclusion from the available and the consumption of oxygen to the cardiac output.

3 | Vasomotion in disease

This chapter describes pathologic incidents in the cardiovascular system and organs during sepsis. Sepsis is used as an example of a disease where vasomotion plays a role.

Sepsis is a condition, that develops on behalf of systemic inflammatory response syndrome (SIRS) with pressence of an infection or bacteria in the tissue, within the body which triggers an immune response. This response often overburdens the immune system, to fight the inflammation or bacteria. The infection or bacteria can be anywhere in the body's tissue. Some of the normal macrohaemodynamics of sepsis are abnormal body temperature, abnormal heart rate, oxygen extraction and abnormal blood pressure.[6, 7] Sepsis is increasing condition in the population. Different studies suggest estimates of the incidence of sepsis, but the identification of diagnosis of sepsis can vary, why the numbers may also vary from place to place.[8, 7] The Dr. Foster Organisation found an increase by 53% from 1996 to 2002 in the hospitals in the United Kingdom. Causes for the increase in incidence can be due to the increasing elderly population, with cronic conditions undergoing invasive procedures [8]. Sepsis is often associated with three stages, sepsis, severe sepsis and septic shock. This is illustrated in figure 3.1.

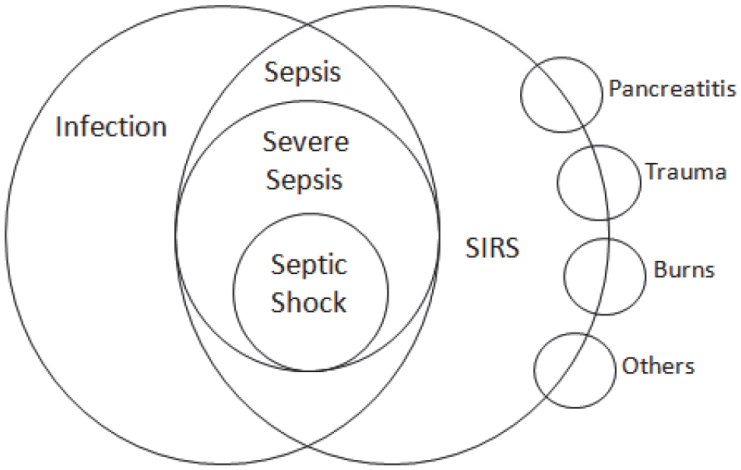

Figure 3.1: Relation between SIRS and infection. Showing the stages in sepsis and some of the causes of SIRS which include pancreatitis, trauma, burns etc.[7]

3.1 Sepsis

Under the stage of sepsis several things happen, mainly to the micro circulatory system at the capillary level, that leads to impaired homeostasis in the body. Infection or other bacteria that is responsible for causing some irregularity is present in the blood and in

the tissues around the vessels. Among the first things that happens when the body encounters an infection, white blood cells are recruited to release molecules that will fight the infection. Molecules that interact with the endothelial in the blood vessels, like nitric oxide (NO), are released. The interaction causes the vessels to dilate to increase the blood vessel diameter and permeability. The increased diameter slows down the blood flow, which causes a drop in blood pressure. Also the vessels permeability is increased. This reaction happens multiple places in the body where there is infected tissue present and will cause systemically vessel dilation. The characterization of sepsis is SIRS as a result of infection.[8, 7]

3.2 Severe sepsis

When the permeability of the vessels is increased there will be more fluid in the tissue and the cells will get less oxygen because the oxygen has a harder time to get to the demanding tissue. Also the endothelial of the vessels will get damaged when the white blood cells try to destroy the pathogens. This triggers coagulation and clotting is formed in the damaged areas in the blood vessels. These clots can break off into the blood and cause further harm eg. stroke. At a point the damaged vessels leads to more leakage, because there will be a point where the coagulation cannot keep up. Organs will start to dysfunction at this stage. The characterization of severe sepsis is presence of sepsis with organ dysfunction and hypoperfusion is often included in this state. The mortality rate for patients with severe sepsis are about 25 to 30% [8, 7].

3.3 Septic shock

Septic shock occurs when the body has undergone sepsis for a greater duration of time. This stage is characterized by a condition with hypotension even after adequate fluid resuscitation is given. Because of lactic acidosis the cells are not getting a sufficient supply of oxygen and therefore the cells will begin to die. This can lead to a very dangerous state, where organs begin to fail because they get to damaged to function. When multiple organs get damaged the state in septic shock reaches multiple organ failure also called multiple organ dysfunction syndrome (MODS)[8, 7]. The mortality for patients with septic shock are in the region of 40 to 70% [7].

4 | Infrared Thermal Imaging

The following chapter will include an introduction to infrared imaging, where some general concepts and physical principals will be explained. Furthermore it will be elaborated how a device measures infrared radiation.

Infrared imaging is an technique that utilizes infrared radiation emitted from nearly any objects. The existence of infrared radiation was first discovered in 1800 by Sir Frederick William Herschel. His experiments lead to the knowledge that there were a light spectrum beyond the visual spectrum humans are able to perceive.[9, 10]

Infrared thermography is commonly used to calculate surface temperatures and important concepts in the understanding of this are heat and temperature. Temperature is a measure for the internal energy within an object and can be defined as the average kinetic energy of the object. Heat is the energy that passes from a warm object to another colder object. A warm object will decrease in internal energy and a cold object will increase due to the temperature difference and therefore the heat transfer. In the human body, a constant temperature is keep, due to several factors and therefore the temperature will not decrease even though a heat transfer to the surrounding environment occurs. The environmental temperature do have an impact on how large the heat transfer gradient is. If a body is in a cold environment, the emitted heat will be greater than the absorbed. In the same way, if the environment is much warmer than 37°C, a greater absorption than emission will occur and the body will increase in temperature.[9]

4.1 Measuring thermal energy

The theory of the black body is important to understand the absorption and emission of light relative to temperature, because the theory of the black body is used to describe the laws of infrared radiation and its relationship to temperature. The black body is an ideal perfect emitter of infrared radiation because it absorbs all electromagnetic radiation permitted to it, and it emits the same amount of radiation as it absorbs, the absorption and emission are both equal to one. Spectral emissive power, also denoted E_λ is the energy emitted by a surface in relation to time and range of wavelength. Figure 4.1 shows an graphical illustration of spectral emissive power of the black body for specific wavelengths when the temperature changes. [9]

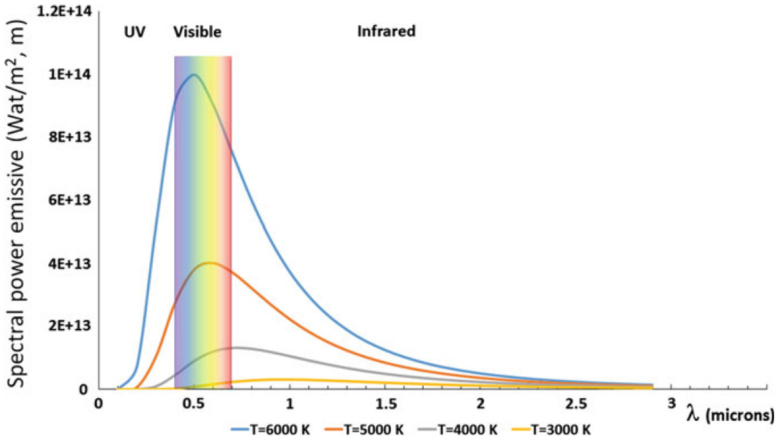

Figure 4.1: Spectral power emissive as a function of wavelength for different temperatures [9]

The knowledge of this principle helps in the understanding of how infrared radiation behaves, and how temperature affects the wavelength of the signal. The radiation from the human body which has a temperature at 37°C emits the maximum energy of 9.3μm, which means that most of the radiation is in the far infrared spectrum.[9]

Physical laws including Wien's displacement law and Stefan-Boltzmann's law are important for explaining how the infrared radiation behaves at different temperatures. [9]

Wien's displacement law tells that the wavelength of the peak of the black body radiation curve decreases as the body temperature increases. This law can be used to describe different wavelengths according to the temperature of the black body which emits the radiation. Wien's law has the following equation:

$$\lambda_{max} = \frac{a}{T} \tag{4.1}$$

In Wiens displacement law 'a' denotes the Wien's displacement constant, this constant has the value $2.897 * 10^{-3} mK$. 'T' denotes the absolute temperature in kelvin. 'λ_{max}' denotes the wavelength of emission peak with unit in meters.[9]

Stefan-Boltzmann's law tells that small changes in temperature will lead to big changes in emissive power. This is seen in Stefan-Boltzmann's equation because it states that the total emissive power is proportional to the fourth power of the absolute temperature. [9]

$$E = \varepsilon * \sigma * T^4 \tag{4.2}$$

In Stefan-Boltzmann's equation 'E' denotes the total emissive power with unit W/m^2. 'σ' denotes the Stefan-Boltzmann's constant, this has a value of $5.67 * 10^{-8} W/m^{-2} K^{-4}$ and 'T' is the temperature in kelvin. 'ε' denotes the emissivity and is normally not a part of the Stefan-Boltzmann's law, but part of the modified Stefan-Boltzmann's equation, because it is used for calculation of temperature in most thermal cameras. Emissivity is different for all materials. Skin have an emissivity between 0.95 to 9.99, why these values typically are used when assessing the temperature of the skin of the human body with thermography. This law is important when considering infrared thermography because the sensitivity when calculating the temperature from the emissive power is big. [9]

Region of interest

Region of interest (RIO) is an important consideration when doing measurements with thermal imaging. One of the reasons why this is an important aspect is because it is the RIO that lays the foundation of the data that goes into the statistical analysis. A minimum of 25 pixels is recommended for the RIO to reduce error in the data. To get the best measurement the RIO should be filling most of the image to get the best thermal data and better resolution in the area you want to measure.[9]

Thermal cameras

The radiation emitted from an object is focusing the RIO onto an array of detectors via a lens in the thermal camera. The array is also called the focal plane array and consists of typically $384 * 288$ to $1024 * 768$ single microbolometers.[11] The radiation emitted to the detectors generates an electric output proportional to the radiation. The output is then undergoing amplification before further signal processing that digitalizes the signal into pixels. This allows the final output signal to be viewed as a temperature for the object on an monitor, this is also illustrated on figure 4.3. [10]

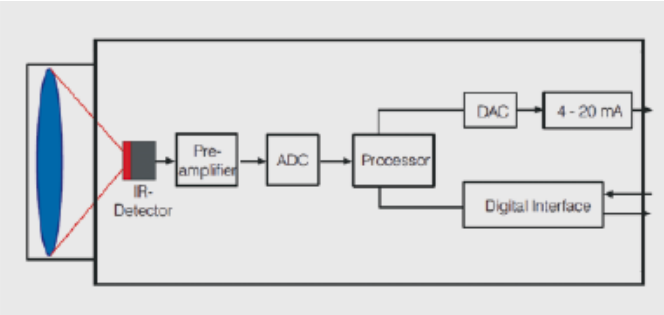

Figure 4.2: Simplified block diagram of an standard infrared camera.[10]

The infrared radiation is made into an electrical signal in the camera, this data can be used in calculating the temperature for an object by knowing certain variables and putting these into Stefan Boltzmann's equation 4.2. The emissive power denoted E, is the radiation that the detector in the camera is getting. The variables σ are known and

ε is specified for the object that is being measured, eg. the human skin with emissivity between 0.95 to 0.99. The temperature are then the only variable to calculate and this is done for each pixel in the image to make up the complete thermal image of the object. Each pixel will be representing one thermal data. [9]

4.2 Physical principals

Any object above absolute zero emits energy-electromagnetic radiation depending on its temperature. Absolute zero is $0K$ or $-273.16°C$. To put that into perspective the human body has a temperature around 37°C.[9, 10]

Electromagnetic radiation is a propagation of energy trough a medium without the transportation of mass. An electromagnetic wave is made of the relationship between frequency f, wavelength λ and the speed of light c. This is stated in the equation of wave motion.[9]

$$\lambda = \frac{c}{f} \tag{4.3}$$

Depending on the frequency and wavelength certain characteristics arise from what is called the electromagnetic spectrum. The electromagnetic spectrum is the electromagnetic energy that is emitted. This extends from radiation of low energy such as radio waves and infrared, to waves of higher energy in form of eg. X-rays. A graphical representation of the electromagnetic spectrum can be seen on fig. 4.3.[9]

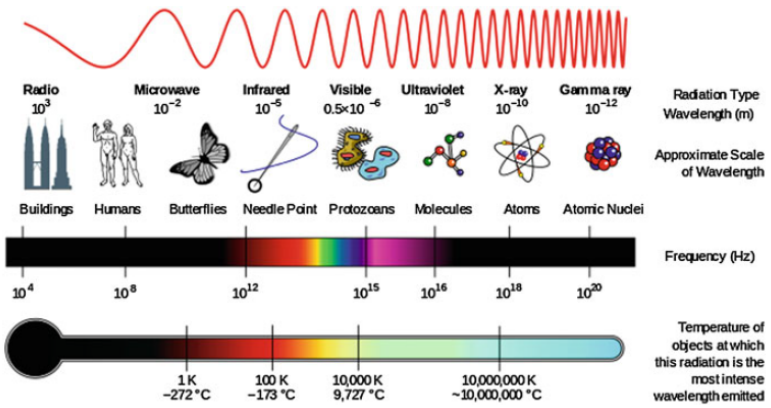

Figure 4.3: The electromagnetic spectrum with wavelength, emitters, frequency and temperature.[9]

Infrared radiation is also known as thermal radiation because of the relationship between temperature and infrared radiation. Temperature of the human body permits radiation in the infrared spectrum, but objects of much higher temperature are capable of emitting radiation in the visible and UV spectrum. This has to do with the difference between object and environmental temperature. If the temperature of these are relatively close to each other, the radiation emitted will be within infrared wavelengths. Infrared radiation has a wavelength from 769 nm to 1 mm. Objects emit more radiation in some region

regions compared to others. Because of this is the infrared spectrum classified in the three regions, near, middle and far infrared. Near is between 769 nm and 2.5 μm, middle 2.5 μm to 50 μm and far 50 μm to 1 mm. The human body emits most radiation in the far infrared part, and most thermal cameras are build with this in mind. Near and middle cameras are used to measure gases.[9]

5 | The use of infrared imaging in vasomotion

In the following chapter an introduction to different techniques of measuring vasomotion will be giving. Here their methods and applicability for measuring vasomotion will be presented, with main focus directed towards thermal imaging as applied technique.

5.1 Techniques of measuring vasomotion

For some time it has been the interest of scientists and health care professionals to get a better understanding of the mechanisms that control and regulate local blood flow in the microcirculatory system[12, 13, 2, 14]. Visualization of the vessels in the skin and the way these behave can be important for assessment of stages of sepsis as mentioned before in chapter 3, but also in peripheral vascular disease, the results of skin reconstructive surgery, wound and ulcer management.[14, 7]

For measuring regulation in the peripheral blood flow, it is assumed that these oscillating changes are the source of thermal waves propagating from microvessels toward the skin's surface. Especially thermal imaging uses this concept.[13] Furthermore a correlation between skin temperature in fingertips and blood flow oscillations has been found[12].

There are multiple different techniques of measuring blood flow in the peripheral circulatory system. Some of these are: capillaroscopy, laser Doppler flowmetry (LDF), laser speckle contrast and orthogonal polarisation spectral imaging. These have been used differently trying to quantify functional aspects of skin vasculature.[14] With Laser Doppler flowmetry being one of the most used[2] and thermal imaging being the new technique of measuring vasoregulation, these will be further exploited[12].

Thermal imaging

In studies made by a Russian group lead by Sagaidachnyi et al. the use thermal imaging has been used to study vasomotion. In their studies they seek to get better understanding of the relationship between blood flow oscillations and temperature oscillations, and see if it was possible to recreate the flow oscillation from temperature recording. Recordings of flow where done by Photoplethysmography and temperature of the skin by thermal imaging. The recordings were made on a small point of the fingertip. Trough their work, five frequency bands were identified as vasomotion activity, and are following: endothelial (0.005–0.02 Hz), neurogenic (0.02-0.05 Hz), myogenic (0.05-0.15 Hz), respiratory origin (0.15-0.4 Hz) and cardiac origin (0.4-2.0 Hz).[13, 12] The choice of using thermal imaging to study vasomotion comes with some advantages. Mainly a larger sample area, but also a higher temporal up to 105 fps and spatial resolution 2048 $\times$ 1536 pixels. In addition

being a non invasive way of measuring vasomotion is to be taken in to consideration.[13]

Laser Doppler flowmetry

In an other study from Geyer et al. vasomotion is investigated trough the use laser Doppler flowmetry as recording technique. In the study vasoregulation variables are sought quantified. LDF is a non invasive approach to measuring changes in vasomotion. The technique register changes in the depth of 1 mm, and works like Doppler ultrasound, utilizing the shift in frequency, but instead of ultrasound, it uses light reflected from red blood cells. This study found the same frequency bands as Sagaidachnyi et al. with minimal difference. Data obtained were analyzed trough spectral analysis. Wavelet transform was used as method instead of the most used fourier, because wavelet analysis offered better resolution to reveal characteristics in the low frequency area.[2] LDF uses a small sample area and the laser probe allows a sampling area as small as 1 mm^3.[15]

5.2 Summarizing

Both Geyer et al. and Sagaidachnyi2017 et al. managed to show spectral components relating to vasomotion. The techniques both uses an non invasive approach, even though the methods are different when measuring red blood cell count compared to temperature. The use of thermal imaging as the method of measuring vasomotion offers interesting opportunities. Larger sampling area would allow interpretation and study of a more global tissue area. Along with the resolution of thermal imaging cameras, this makes thermal imaging the choice of measuring technique to be used in this study.

Part II

Experimental method

6 | Study setup

In this study the peripheral circulation is observed to investigate if there are changes in microcirculation during partial occlusion of blood supply. Infrared imaging is used to measure the temperature changes in the skin of the hand, which is used as an indicator for peripheral circulation.

To see if there are changes in the microcirculatory system depending on flow levels in the macrocirculatory system, the test is set in two conditions. The first measurement of the hand, which is done under normal conditions, is used as a control measurement. The second measurement of the hand is done during a partial occlusion of the blood supply. The partial occlusion of the arm leads to a lower oxygen supply which leads to ischemia, and is used as a way to mimic sepsis. The reason to do a 50% restriction of blood, is due to the intend of creating a high level of ischemia without forcing to much discomfort on test subjects.

By first taking the control measurement under normal conditions, the carry-over effect of the occlusion is avoided. It also enables to take both measurements of each subject straight successively, what reduces inaccuracies within the setup of both experiments for each subject. Therefore a special setting, which is shown in fig. 6.1 is assembled in the Regionshospital Nordjylland in Hjørring.

6.1 Subjects

Four healthy subjects within the age of 22 - 52, three men and one female were recruited for this experiment. The experiment is done as a pilot study, why it is presumed that the sample size of four is sufficient. The research focuses on assessing the microvasular system with the hand as a window on healthy subjects. Therefore certain inclusion and exclusion criteria have been formed:

Inclusion criteria

- Subjects should have at least one hand to perform the measure on
- The cuff should be able to fit the arm circumference
- The subject should be able to sit still for a greater extend of time

Eksclusion criteria

- Health conditions that sets the subject in risk of injury when conducting the experiment like high blood pressure.
  - Systolic blood pressure over 140

  - Diastolic blood pressure over 90

- Age under 18 years old
- Age over 60 years old
- Obesity to a greater extend
- Diseases that triggers tremors

6.2 Test setting

The subject will be placed in a upholstered chair with adjustable backrest, footrest and armrests, which allows a good positioning of the measured hand, while the subject remain in a relaxed position. Measurement will be carried out on the dominant hand and it must be fixed during the whole test to minimize movement bias. The hand is stabilized with a vacuum pillow which is covered by a micro fiber tissue to get a better background for the images. To provide a more comfortable position of the arm during the experiment the armrest of the adjustable chair is padded with some sheets under the vacuum pillow. A comfortable position in the chair is important, because the subject has to sit still and is not allowed to move during the test for at least 45 min. These precautions only counteract some small movement, and therefore it is important that the subject is focused on sitting still. $37,5 \pm 1,0$ cm over the hand the Xenics Gobi 640 17μm GigE infrared camera is positioned with a tripod. The setup with camera, chair and computer can be seen on fig. 6.1

Figure 6.1: The test setting at the Regionshospital Nordjylland.

The focus is adjusted on the hand from tip of middle finger till wrist. The camera is via a Ethernet cable connected with a laptop, which is used to record the measurements with Xeneth 2.6 software. First the cable connections between the camera, the laptop and the power supply have to be set. Afterwards the camera is turned on and has to warm up for

about 15 min. During this the laptop should be started and the software for taking the measurements is set in operational readiness.

When the preparation of the test setting is done, the preparation for the subject can begin. At first the blood pressure of the subject is measured on the dominant arm. The blood pressure is measured three times while the subject is sitting relaxed on a chair. Mean systolic blood pressures is calculated. To get the total occlusion pressure (TOP) the mean has to be multiplied by 1.3. To reduce the blood flow in the arm to 50% during the measurement within the second condition, the arm is cuffed with 30% of the TOP.[16] Then the cuff is affixed at the subjects dominant arm without tighten it. After that the subject can take place in the chair and the hand can be stabled with the vacuum pillow. The vacuum generator is attached to the pillow for giving the hand more stability. Next the camera needs to be positioned $37,5 \pm 1,0cm$ over the hand. The focus has to be adjusted so the distance is taking in to consideration, to make sure the image is sharp.

If the camera is stable and the filename is modified according to the subject, the first measurement can be started for 20 min. The time needs to be measured by a stopwatch. During the whole experiment the subject is not allowed to move or speak to minimize movement bias. Directly after the first measurement the cuff on the arm of the subject is tightened with the calculated value. The pressure of the cuff should be observed during the whole measurement and if necessary adjusted.

To guide the conductors of the experiment, an experimental protocol had formed and should be followed during the experiment. The experimental protocol can be seen in chapter A.

6.3 Software setting

To interface the Xenics camera, Xeneth 2.6 software was used and settings were controlled from here. Sampling rate for the thermal imaging camera was set to the lowest possible at $50 * \frac{1}{8}$. This should be sufficient according to the Nyquist theory, when the frequencies of interest lies within $0.005Hz - 2Hz$ as presented in section 5.1. Ambient temperature of the room was set to 25° and emissivity to 1.

Part III

Data analysis

7 | Preparation of the data

Dividing the data into frames

The data acquired from the thermal camera using the Xeneth 2.6 software gives an xvi file as output for each recording. These files was loaded and read into Matlab R2017b as an uint16 vector file. Before the frames could be separated from the xvi file, the header in front of the files needed to be excluded. The header contained 307729 data points. With the header removed, the frame separation could be carried out. This was done by first calculating the size of one frame. When knowing that each frame would have the dimensions of 640x480 pixels, the size of one frame would correspond to 307200 data points for each frame. It should be noticed that each frame also contained a 16 bit header, so this should be added to the size of each frame. The number of frames was calculated by dividing the length of one frame by the entire length of the data file containing all frames, without the header. By this calculation it was known how many frames the file contained. The data points for each frame were reshaped from a vector into a matrix and verified by showing the images. The images contain the pixel intensities of values from 0 to 65535, which is corespondent to the size of the uint16 byte file.

Figure 7.1: Image of frame one from a subject

8 | Regions of interest

The regions of interest (ROI) were chosen as pixel locations in the image on specific places of the hand. ROI were selected on behalf of getting a full representation of the hand, to investigate the regions which show the most significant difference when computing the statistical test. Regions in the fingertips and nail folds are areas where it is easy to access the microcirculatory hemodynamics of the human body according to [17]. This region should therefore be expected to give some information on the changes in capillaries which can be an effect of vasomotion.

The original image 7.1 is showing the hand but not with very good contrast. To easier choose ROI, the original image was converted to a gray scale image to improve the contrast in the image, this can be seen in 8.1.

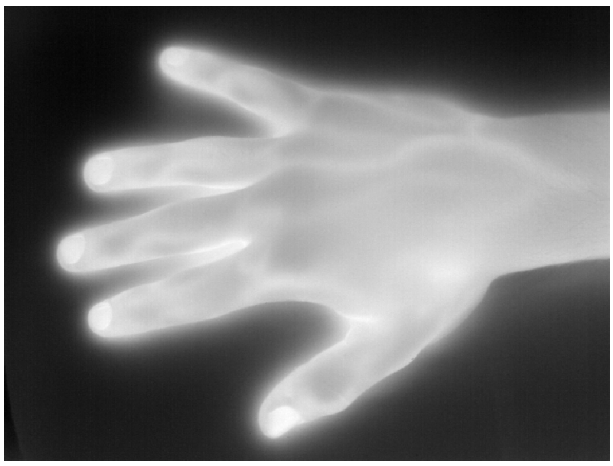

Figure 8.1: First thermal image of the thermal image series for subject 1, grayscale image

With the improved contrast, 28 ROI from the hand were chosen on the first image of the thermal image series, by finding the coordinates of the pixels on the image. The regions are illustrated on 8.2. The localization of the regions is originating from the fingertips and elongating down the hand to the beginning of the wrist. Each region gives an pixel intensity value from one pixel of the image. Further more the mean of the chosen pixel value and the neighbor pixels, a total of nine pixels, is calculated for each region to get a more general value for the specific region.

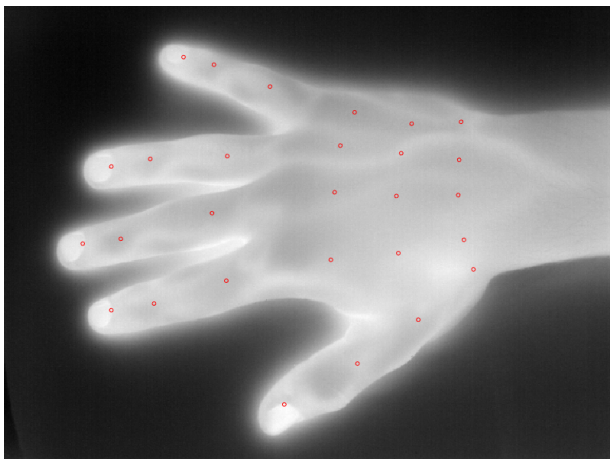

Figure 8.2: First thermal image of the thermal image series for subject 1, with ROI of interest plottet on 28 areas of the hand represented as red circles

The regions are constant for the whole image series for each measurement, assuming that the subject was sitting still during the whole measurement. The regions also account for both the uncuffed and cuffed conditions for each subject, assuming that the position of the hand was at the same position in both conditions. Iterating over the image series saving ROI into a cell array with data points for each ROI, a vector for the each of the 28 regions was made to give the pixel intensity variations over the whole measurement. An example of the pixel intensities for subject 1 is shown on image 8.3

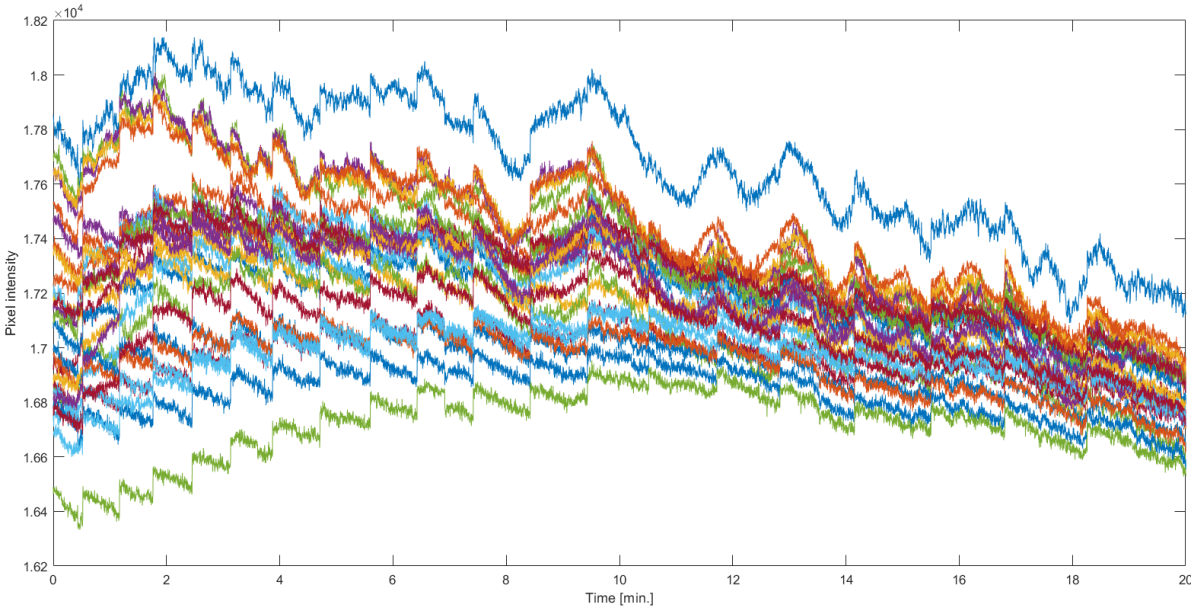

Figure 8.3: Pixel intensity for all 28 ROI, plottet from subject 1, for the entire thermal image series of a measurement

8.1 Reason for unexpected data

Because of the data seen in figure xx in section zz, a real representation the natural occurrence, and therefore it is assumed that the greater shifts is due to a technological limit. Because of this assumption it is chosen to further investigate the buildup of thermal cameras and look into other papers, to see if they have meet same difficulties.

8.1.1 Thermal pixel drift

In a study by Eriksen et al. where thermal imaging was assessed as use for measuring temperature of electrical systems, data recording showed similar behavior as recording in this study. They clearly state that two types of noise is present in their recording. One being white noise from the radiation detector and electronics, and another being a low frequency technical noise. To compensate for these artifacts, a moving average filter was applied.[18]

Thermal cameras are composed of a matrix of microbolometers as mentioned in section section 4.1. Each microbolometer is also known as a pixel detector for thermal radiation.[11, 19] Unfortunately it shows that these microbolometers are really sensitive to noise especially in uncooled cameras. The noise is formed because each microbolometer has a different response to the same infrared excitation. Furthermore it is assumed by some that this response changes linear[11]. This drift in each microbolometer in the focal plane array is also known as non-uniformity. To achieve radiometric precision the camera has to make a correction for this drift called non-uniformity correction. A common way to recalibrate bolometers is to move a shutter in between the lens and the focal plane array. The shutter has the same color and by statistical calculation it is possible to find the drift for each bolometer and create a new base.[11, 19] This auto-adjustments might be what Eriksen et al. saw in their recordings.

8.1.2 Correction method

After plotting the radiant intensity for each region of interest it is apparent that there are unnatural jumps within the signal shown in 8.4. Those jumps occur in each region of interest at the same time and are shown by a high difference of the values between two frames. The amount of the observed jumps varies between 0 and 20 in the recordings. Furthermore the appearance of the jumps is non-periodic and in each recording at different time points.

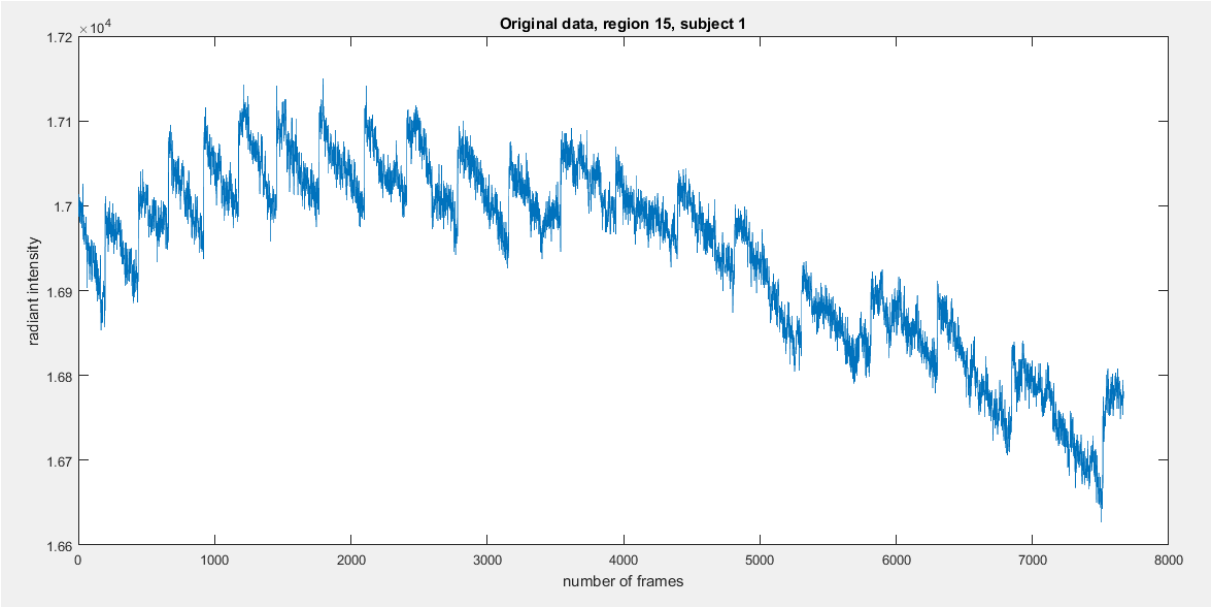

Figure 8.4: The original data of region 15 in the uncuffed recording of subject 1 including 20 jumps.

A continuous wavelet transform out of the raw data shows a magnitude scalogram with high magnitude peaks exactly at the same time points where the jumps are occurring. Due to this falsifying of the magnitude, the results of the data analysis are also falsified. Additionally there is also a drift occurring within each interval between two jumps, which hampers the correct data analysis. To reduce the drift component and the jumps in the signals, the two following correction methods have been compiled, whereby the second one has been implemented.

Method 1: Regression of first interval

The first implemented method is based on the assumption that the drift is equal in each interval. It is also assumed that the thermal camera has been calibrated just before the recording, so the first interval can be used as a reference to calculate the drift component. Therefore a linear regression for the first interval has been made. With the resultant slope m follows the calculation of the drift difference d within the first interval. Due to the assumption, that the drift difference is equal, the slope of the drift of each interval depends on the length of the interval. The slopes have been calculated with equation 8.1.

$$m = \frac{d}{length(interval)} \tag{8.1}$$

To compensate the drift, a straight with the inverse slope and the starting point in the first data point of the interval has been calculated. The middle points between the original data and the new calculated straight build the correction of the data signal. This correction worked within the signal just in several parts and had a lot of weak points where the jumps have been strengthened. Due to the outcome of this method the assumption, that

the drift is equal in each interval has been discarded. [1]

Method 2: Regression of each interval

The second implemented method is due to the failure of the first method based on the assumption that the drift is not equal in each interval. Out of the recorded data the exact drift is indeterminable. Hence a method which tries to fit the separate intervals together without the necessity of the awareness of the real drift component and avoids the suppression of the basic shape of the signal has been chosen. Therefore firstly the linear regressions for all intervals and the corresponding residuals are calculated. The idea is to move the end point of a regression line and the start point of the next regression line together. Thus the middle points between end and following start point are calculated. The alignment of the regression lines is changed, so that the start and end points of all the new created orientation straights fit the middle points, except the first and the last orientation straight. Both fit just one middle point. The start of the first orientation straight is the start point of the regression line of the first interval and the end point of the last orientation straight is the end point of the regression line of the last interval.

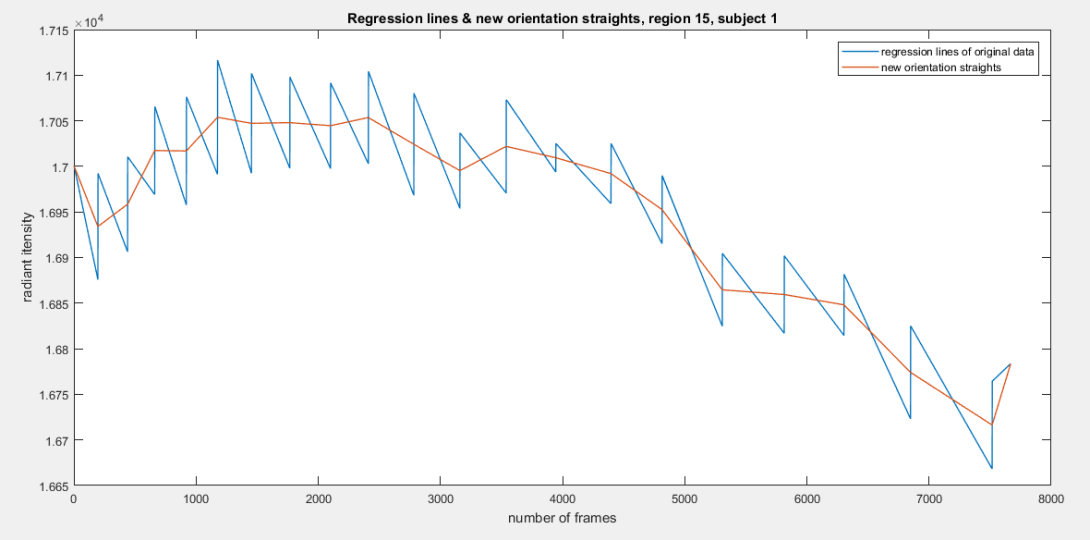

Figure 8.5: Connected regression lines of the original data of region 15 in the uncuffed recording of subject 1 in blue. New created orientation line of the same recording in the same region shown in red.

As shown in figure 8.5 the new orientation straight fits the regression lines together without suppressing the shape of the signal. Subsequently the residuals have been added to the new orientation straight, to sustain the ratio between the data points. Figure 8.6 shows the corrected signal wherein the by jumps separated intervals have been connected and the jumps have been largely corrected.

[1] FiXme Note: figure missing

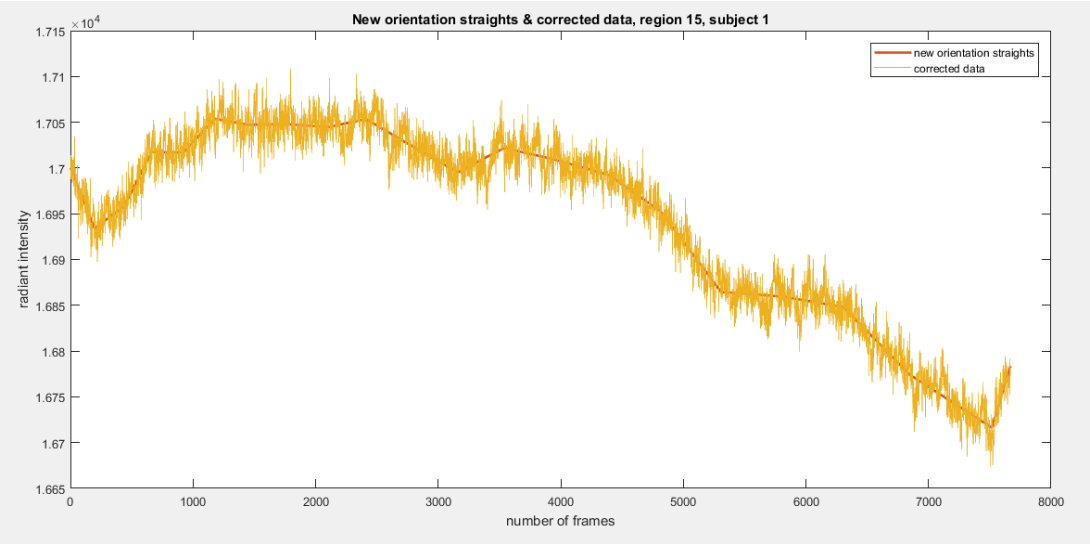

Figure 8.6: Orientation line based on the data of the uncuffed recording of subject 1 in region 15 shown in red. Corrected signal of the same data in yellow.

However, this method still has weak points. The in figures 8.4 - 8.6 shown region of interest is located in the center of the thermal image. Regions which are located in the outer area of the thermal image show a few jumps after the correction which are bigger than before (8.7). These sporadic extended jumps are due to the fact that the thermal image is more unstable in the outer areas than in the center, thus the pixel drift is increasing with increasing distance of the center.

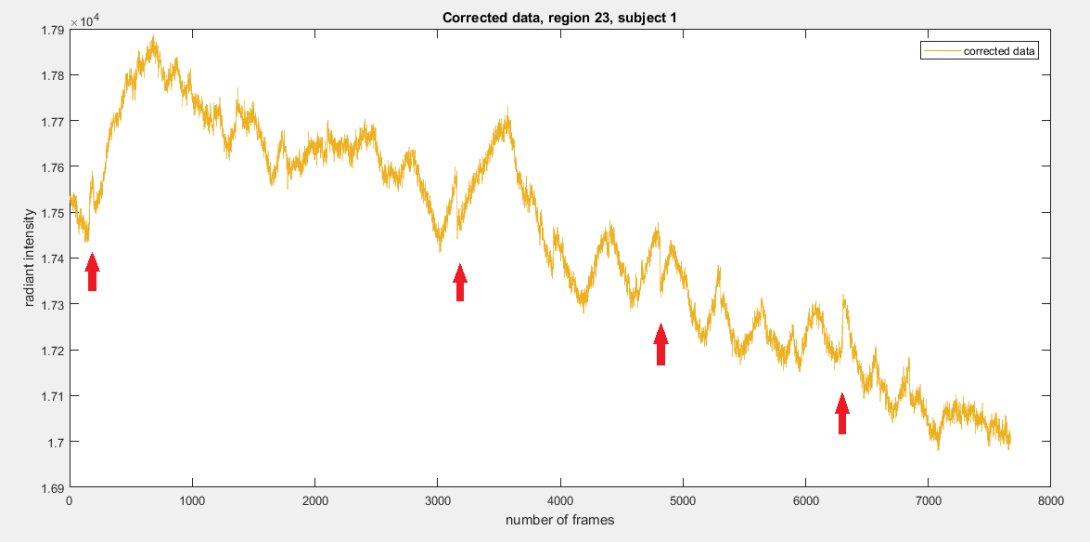

Figure 8.7: Corrected data of the uncuffed recording of subject 1 in region 23 shown in yellow. Red arrows show the jumps in this signal.

8.2 Continous wavelet transformation

The wavelet transform is used to see the frequency components of the signal in the time frequency domain. Wavelet transformation is practical when looking for signals of lower frequencies compared to the normal fourier analysis, because of the bigger resolution in the wavelet analysis. [2] Another drawback of the fourier transform is the loss of time information.

The wavelet transformation is using a variable sized region windowing technique. Long time intervals are used where low frequency information is computed and short time intervals are used where high frequency information is computed. This is represented in figure 8.8.

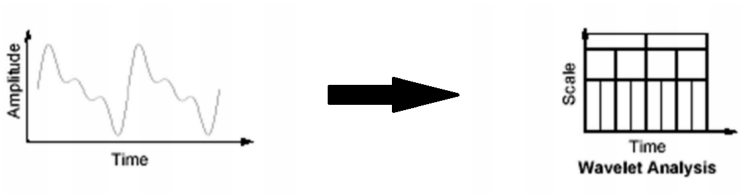

Figure 8.8: Signal to wavelet computation, modified from [20]

The wavelet computes both the scale (s) and position (p) for the wavelet transform.

$$C(s,p) = \int_{-\infty}^{\infty} f(t)\Psi(s,p)dt \tag{8.2}$$

The signal f(t) is convoluted with the wavelet Ψ to get the wavelet coefficients for s and p.

This is done by computing the wavelet of the signal which then is compared to the wavelet for a section at the beginning of the signal. Then C in equation 8.2 is calculated for the section of the signal. The wavelet is shifted to the right and repeated until the entire signal is covered. Then the wavelet is scaled and C is computed for the entire signal again for all scales. [20]

Different wavelets can be used to compute the wavelet transformation. In Matlab the default is the Morlet wavelet.

The general form of the continuous wavelet transform is stated in equation 8.3:

$$W(t,s) \equiv \int_{-\infty}^{\infty} \frac{1}{s^n}\psi * (\frac{\tau - t}{\mathrm{s}})x(\tau)d\tau \tag{8.3}$$

Where $\psi * (\frac{\tau - t}{s})$ is the wavelet and $x(\tau)$ is the signal.[20]

The signal or function is put into the continuous wavelet transformation equation 8.3. The wavelet transform will give a scolargram as an output. In Matlab the function cwt can be used to compute the continuous wavelet transformation by inserting the signal and the sampling frequency. This will give a scolargram as shown in figure **??**. [21] The frequencies in Hz are shown along the y-axis if the sampling frequency is specified, else it will show the normalized frequency in cycles pr. sample. Along the x-axis is the time vector. The scolargram show the magnitude of the signal to show how the frequency in the signal is distributed. A scale to see the size of the magnitude is also implied. An example of a scolargram is given in figure 8.9

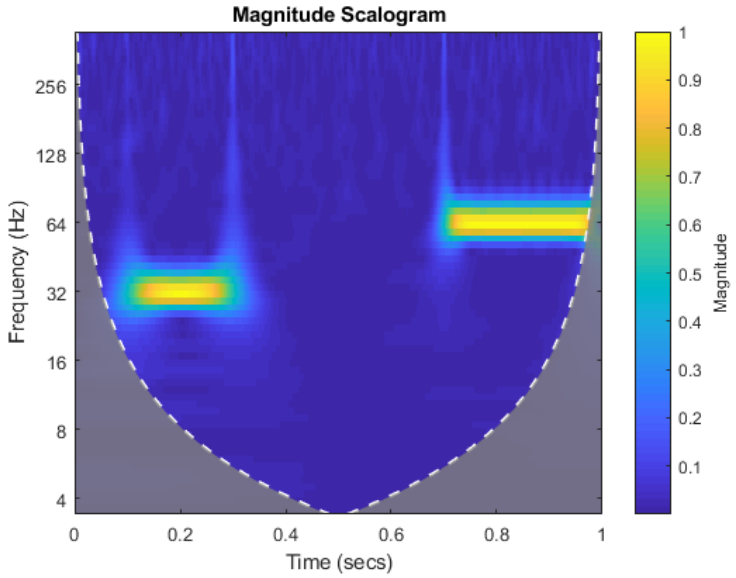

Figure 8.9: An example of a scolargram, showing frequency content at 32 Hz at time approx 0.2 sec and 64 Hx at approx 0.8 sec [21]

9 | paired t-test

The used method of the study design is called in series design. This enable to compare the situation before and after treatment within each subject.

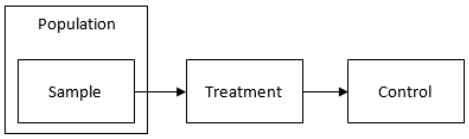

Figure 9.1: The procedure of studies with in series design.

Within this study the arms of the subjects will be cuffed. To avoid any carry-over effect, the measurements on the normal arm will be done first. That means beginning with the control and then the "treatment".

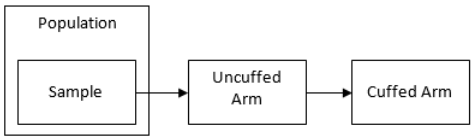

Figure 9.2: The procedure of this study with in series design.

The paired t-test is used to check the difference of means of two conditional samples. This test is usually used to compare "before treatment" and "after treatment". The tested hypotheses are (where $\delta = \mu_1 - \mu 2$)[22]:

- $H_0 : \delta = 0$ no difference between uncuffed and cuffed arm
- $H_1 : \delta \neq 0$ a difference between uncuffed and cuffed arm

In this case, there is a relation between the microcirculatory and the macrocirculatory system shown, if the null hypothesis is rejected.

It is requisite that the sample size of the of both samples is identical.

Following some useful formulas[22]:

- difference within the subjects

$$d_i = x_{i2} - x_{i1} \tag{9.1}$$

  with $i = 1, 2, ..., n$

- mean of the difference

$$\bar{d} = \frac{1}{n}\Sigma d_i \tag{9.2}$$

  with $i = 1, 2, ..., n$

- standard deviation

$$s_d = \sqrt{\frac{\Sigma(d_i - \bar{d})^2}{n-1}} \tag{9.3}$$

- test variable

$$T = \frac{\bar{d}}{\frac{1}{\sqrt{n}}s_d} \tag{9.4}$$

- degrees of freedom

$$n - 1 \tag{9.5}$$

- decision rule for rejecting the null hypothesis

$$|T| > t_{n-1,\frac{\alpha}{2}} \tag{9.6}$$

Bibliography

[1] Bartholomwe EF Martini FH, Nath JL. *Fundamentals of Anatomy and Physiology Ninth Edition*. Pearson, 2012, p. 1272. ISBN: 13: 978-0-321-70933-2.

[2] Mary Jo Geyer et al. "Using wavelet analysis to characterize the thermoregulatory mechanisms of sacral skin blood flow." In: *Journal of rehabilitation research and development* 41.6A (2004), pp. 797–806. ISSN: 0748-7711. DOI: 10.1682/JRRD.2003.10.0159.

[3] Marc Thiriet. "Biology and Mechanics of Blood Flows - Part II: Mechanics and Medical Aspects". In: ().

[4] Abraham Noordergraaf. *Blood in Motion*. 2011.

[5] Ashfaq Hasan. *Handbook of Blood Gas/Acid-Base Interpretation*. 2013.

[6] Robert H. Shmerling Ryszard M. Pluta. "Jama patient page - Sepsis". In: 308.20 (2010), p. 7424.

[7] Saowanee Kanta, Boonyang Plangklang, and Wanchai Subsingha. "World ' s largest Science , Technology & Medicine Open Access book publisher c". In: *Energy Procedia* 56.C (2014), pp. 604–609. ISSN: 9789533070865. DOI: 10.5772/711.

[8] Simon V. Baudouin. *Sepsis: Introduction and Epidemiology*. 2008, pp. 1–2. ISBN: 9781846289385. DOI: 10.1007/978-1-84628-939-2_1.

[9] Jose Ignacio et al. *Application of Infrared Thermography in Sports Science*. 2017, pp. 49–79. ISBN: 978-3-319-47409-0. DOI: 10.1007/978-3-319-47410-6. URL: http://link.springer.com/10.1007/978-3-319-47410-6.

[10] Optris. "BASIC PRINCIPLES of non-contact temperature measurement". In: (2009), pp. 1–7. URL: www.optris.com/applications?file=tl%7B%5C_%7Dfiles/pdf/.../IR-Basics.pdf.

[11] Robert Olbrycht and Boguslaw Wiecek. "New approach to thermal drift correction in microbolometer thermal cameras". In: *Quantitative InfraRed Thermography Journal* 12.2 (2015), pp. 184–195. ISSN: 21167176. DOI: 10.1080/17686733.2015.1055675. URL: http://dx.doi.org/10.1080/17686733.2015.1055675.

[12] a a Sagaidachnyi et al. "Determination of the amplitude and phase relationships between oscillations in skin temperature and photoplethysmography-measured blood flow in fingertips." In: *Physiological measurement* 35.2 (2014), pp. 153–66. ISSN: 1361-6579. DOI: 10.1088/0967-3334/35/2/153. URL: http://www.ncbi.nlm.nih.gov/pubmed/24399251.

[13] A A Sagaidachnyi et al. “Thermography-based blood flow imaging in human skin of the hands and feet: a spectral filtering approach”. In: *Physiological Measurement* 38.2 (2017), pp. 272–288. ISSN: 0967-3334. DOI: 10.1088/1361-6579/aa4eaf. URL: http://www.ncbi.nlm.nih.gov/pubmed/28099162%7B%5C%%7D5Cnhttp://stacks.iop.org/0967-3334/38/i=2/a=272?key=crossref.169506a8780bc72b4d9d219e09a28a32.

[14] Wei Min Liu et al. “Reconstruction of thermographic signals to map perforator vessels in humans”. In: *Quantitative InfraRed Thermography Journal* 9.2 (2012), pp. 123–133. ISSN: 21167176. DOI: 10.1080/17686733.2012.737157.

[15] R Matthew Brothers et al. “Methodological assessment of skin and limb blood flows in the human forearm during thermal and baroreceptor provocations”. In: *J Appl Physiol* 109 (2010), pp. 895–900. ISSN: 8750-7587. DOI: 10.1152/japplphysiol.00319.2010.âĂŤSkin.

[16] J. Grant Mouser et al. “A tale of three cuffs: the hemodynamics of blood flow restriction”. In: *European Journal of Applied Physiology* 117.7 (2017), pp. 1493–1499. ISSN: 14396319. DOI: 10.1007/s00421-017-3644-7.

[17] M. L. Iabichella, E. Melillo, and G. Mosti. “A Review of Microvascular Measurements in Wound Healing”. In: *The International Journal of Lower Extremity Wounds* 5.3 (2006), pp. 181–199. ISSN: 1534-7346. DOI: 10.1177/1534734606292492. URL: http://journals.sagepub.com/doi/10.1177/1534734606292492.

[18] Anders Eriksen, Dominik Osinski, and Dag Roar Hjelme. “Evaluation of thermal imaging system and thermal radiation detector for real-time condition monitoring of high power frequency converters”. In: *Advances in Manufacturing* 2.1 (2014), pp. 88–94. ISSN: 21953597. DOI: 10.1007/s40436-014-0066-1.

[19] Alejandro Wolf, Jorge E. Pezoa, and Miguel Figueroa. “Modeling and compensating temperature-dependent non-uniformity noise in IR microbolometer cameras”. In: *Sensors (Switzerland)* 16.7 (2016), pp. 1–13. ISSN: 14248220. DOI: 10.3390/s16071121.

[20] Cintia Bertacchi Uvo. “Fourier and Wavelets Transforms”. In: (1995), pp. 1–19.

[21] MathWorks. *Continuous 1-D wavelet transform*. 2017. URL: https://se.mathworks.com/help/wavelet/ref/cwt.html?searchHighlight=cwt%7B%5C&%7Ds%7B%5C_%7Dtid=doc%7B%5C_%7Dsrchtitle (visited on 01/01/2017).

[22] Yadolah Dodge. *The Concise Encyclopedia of Statistics*. 2008. ISBN: 978-0-387-32833-1. URL: https://link.springer.com/referencework/10.1007/978-0-387-32833-1.

A | Protocol

Experimental Protocol

Experiment

Study of temperature oscillations in the peripheral circulation with infrared thermography

Formalities

Date:	17.10.2017 and 18.10.2017
Place:	Regionshospital Nordjylland in Hjørring
Conducted by:	Toby Waterstone, Christian Mortensen, Annabel Bantle, Andrei Ciubotariu

Background

Aim:	The aim of the experiment is to measure vasomotion in the hand in two conditions	
Type of study:	Quantitative research	
Subjects:	Number of subjects:	4
	Inclusion criteria:	• Subjects should have at least one hand to perform the measure on • The cuff should be able to fit the arm circumference • The subject should be able to sit still for a greater extend of time
	Exclusion criteria:	• Health conditions that sets the subject in risk of injury when conducting the experiment like high blood pressure. • Age under 18 years old • Age over 60 years old • Obesity to a greater extend • Diseases that triggers tremors

Test Requirements

Materials:	Xenics Gobi 640 17μm GigE Infrared camera with power cord, Tripod, Cuff, Chair, Computer with recording software and power

Experimental Protocol

	cord, Vacuum pillow, Vacuum pump, Stopwatch, Ethernet cable, Computer.
Setup:	
Preparation:	1. The camera has to warm up for 15 min. 2. During this laptop, software and all cable connections should be set in operational readiness.
Procedure:	1. Systolic pressure is measured and mean is calculated 2. Pressure to be used in cuff is calculated 3. The cuff is affixed at the subjects dominant arm without tighten it. 4. The subject can take place in the chair. 5. The hand is put on the vacuum pillow. 6. The vacuum pump is attached to the pillow. 7. The camera needs to be positioned 37.5 cm over the hand with the focus adjusted. 8. If the camera is stable, the first measurement can be started for exact 20 min. 9. Save file as subject_number of subject. 10. Tighten the cuff on the arm of the subject with XXX, without moving the subjects hand. 11. The second measurement can be started for exact 20 min. 12. Maintain same pressure for 20 min. 13. Save file as subject_number of subject_cuff

Table A.1: Table of blood pressure.

Subject number	1. systolic pressure	2. systolic pressure	3. systolic pressure	Mean pressure	30 % of TOP
1	141 mmHg	138 mmHg	137 mmHg	138.6 mmHg	54.08 mmHg
2	102 mmHg	102 mmHg	102 mmHg	102 mmHg	39.78 mmHg
3	155 mmHg	147 mmHg	146 mmHg	149.3 mmHg	58.24 mmHg
4	138 mmHg	145 mmHg	135 mmHg	139.3 mmHg	54.34 mmHg